ELSEVIER

Nuclear Instruments and Methods in Physics Research B 149 (1999) 490–500

NIM B
Beam Interactions with Materials & Atoms

Multi-hit detector system for complete momentum balance in spectroscopy in molecular fragmentation processes

I. Ali [a,c,*], R. Dörner [a], O. Jagutzki [a], S. Nüttgens [a], V. Mergel [a], L. Spielberger [a], Kh. Khayyat [a], T. Vogt [a], H. Bräuning [a], K. Ullmann [a], R. Moshammer [b], J. Ullrich [b], S. Hagmann [c], K.-O. Groeneveld [a], C.L. Cocke [c], H. Schmidt-Böcking [a]

[a] *Institut für Kernphysik, Universität Frankfurt, August Euler Str. 6, D60486 Frankfurt, Germany*
[b] *Gesellschaft für Schwerionen Forschung, D64291 Darmstadt, Germany*
[c] *Department of Physics, Kansas State University, Manhattan, KS 66506-2604, USA*

Received 19 May 1998; received in revised form 14 September 1998

Abstract

A multi-hit detector system has been developed capable of measuring the complete momentum vectors of all ionic fragments after the dissociation of complex molecules induced by photon, electron or ion impact. The fragments are collected in an electrostatic field and detected with a position-sensitive micro-channel plate detector using a fast timing delay-line readout. The detector has a position resolution better than 0.2 mm and can resolve fragments with arrival times separated by at least 5 ns in time. We illustrate the features of this new detector with first measurements for the collision process $He^{1+} + N_2 \rightarrow He^0 + N^{p+} + N^{q+} + (p+q-1)e^-$ and the complete momentum profile of all reaction products. A momentum resolution of 10 a.u. perpendicular to the beam derived from the time-of-flight (TOF) and 20 a.u. perpendicular to the beam derived from the position on the detector have been obtained using a room temperature target system for nitrogen molecules. An angular resolution of $\pm 5°$ is obtained.

1. Introduction

The study of the molecular fragmentation has been established as an important tool in the field of physics and chemistry to investigate the dynamics of a molecular dissociation process. The kinematically complete detection of the correlated emission of fragments in the dissociation process of a molecule yields direct information on the molecular structure.

Depending on the number (n) of final fragments there are $3n+1$ (including the Q-value of the reaction) kinematical parameters for each fragmentation process. Because of momentum and energy conservation the number of independent parameters is $3n+1-4=3n-3$. In order to obtain complete information on the kinematics of the fragmentation process thus $3n-3$ momentum parameters have to be measured.

* Corresponding author. Fax: +1 785-532-6806; e-mail: imadali@phys.ksu.edu

0168-583X/99/$ – see front matter
PII: S0168-583X(98)00916-1

Most of the experimental investigations in the past studying such fragmentation processes were performed with the molecular target at rest in the laboratory system. For these investigations different techniques such as time-of-flight (TOF), electrostatic angular spectrometer systems and ion–ion coincidence techniques were exploited to measure the kinematics of the molecular fragments [1–6]. The information on the dissociation process is derived from the kinetic energy and emission angle of the detected fragments. Another interesting technique was used by Vager et al. [7]. Here a fast (MeV) molecular beam from electrostatic accelerator dissociates in a thin foil or in gas; collision fragments are fast in the laboratory frame and can easily be detected down-stream with specially developed multi-particle position and time sensitive detectors [8,9]. Through detection of position and TOF of the Coulomb-exploding fragments, the stereochemical structure of the molecular ions constituting the incident beam can be deduced. This technique to study the molecular structure is called the Coulomb-explosion technique. The Coulomb-explosion technique has been successfully applied to study the structure of molecules that are difficult to study using the traditional photon spectroscopy techniques because of the extremely weak emission or absorption lines. However, the energy of the Coulomb-exploding fragments in a foil is influenced by additional effects such as wake forces, electron screening, multi-scattering etc., which complicates the derivation of dissociation energies and anisotropies from the data thus its application is sometimes limited.

The most recent experimental approach to study fragmentation processes of molecular targets utilizes modern multi-hit detection capability. In the most frequently used version all ionic fragments are projected by an electrostatic field onto a single not position sensitive detector. This multi-hit detection systems is only capable of measuring the TOF difference between the fragments arriving on the same detector. That means from these measurements only the momentum components in one dimension namely the direction of the extracting electrostatic field can be derived, providing important but non-complete information on the total momentum balance in a multiple molecular fragmentation process [10–12].

Very recently first results have been reported using a position-sensitive multi-hit detection system, which yields information on the complete momentum balance in molecular break up. The position information is obtained by using a wedge-and-strip (W-S) anode [13,14] or a pixel read-out system [15,16]. A detector with a W-S anode can have a position resolution better than 0.1 mm and a time resolution of the first arriving charged fragment of better than a nanosecond. However, for multi-fragment detection the system is not ready to separate the second arriving fragment for about 200 ns from the pulse the first fragment has generated, since the charge collection from the W-S anode by standard electronics needs about this time. A pixel detector has a much faster multi-hit response for parallel read-out of the pixels for the fragments. It can resolve particles which arrive within a time interval longer than the electronic time resolution of typically 10 ns. However, the position resolution of such a pixel detector is limited by the pixel size of typically (1–2) mm.

In this paper we report on a position-sensitive multi-hit detection system (PMDS), which is based on a very fast delay-line position read-out. A multi-channel-plate (MCP) detector equipped with a delay-line-anode can have a position resolution better than 0.1 mm. Two fragments which arrive with a very short time difference on the detector at different positions can principally be detected as known from the pixel detector [15,16]. This system can only detect the second fragment only if the two detector signals are separated in time by more than 10 ns due to the current limits of fast timing electronics. From the measured TOF and position of all the emitted fragments this new detection systems provides a detailed insight into the momentum balance of the fragmentation process. By applying high extraction voltages the emitted fragments can be projected on the detector in a wide solid angle of virtually 100% from 4π.

The PMDS developed in this work was tested with the diatomic break-up process of N_2 molecules in capture collisions with 200 keV He^{1+}-projectiles. The fragmentation of N_2 was chosen to demonstrate the efficiency and high resolution of

the multi-hit system, because N_2 explodes into similar charged fragments such as two N^{1+} or two N^{1+} ions (see the reaction channels in Eqs. (8)–(10)). These fragments arrive on the detector within very short time differences. Thus this case is helpful for testing the limits of the two-pulse time resolution of the system. The charge-exchanged outgoing He^0 projectiles were detected in triple-coincidence with the N^{q+} two fragments by a position-sensitive channel plate detector providing a precise timing for the collision.

2. Experimental set-up

The schematic of the experimental set-up is shown in Fig. 1. The experiment was performed at the 2.5 MeV Van-de-Graaff-accelerator at the Institut für Kernphysik der Universität Frankfurt. The incoming 200 keV He^{1+} beam was collimated to a beam spot of less than 0.05 mm^2 by two pairs of collimators. The He^{1+} beam intersected a diffusive N_2 beam (300 K) effusing from a hypodermic needle. The resulting ions and ionic fragments from the collision process were accelerated by an electrostatic field (400 V/cm) over 20 mm before they drifted in a field-free region 40 mm toward the channel plate detector. The lengths of the drift and acceleration regions were chosen to ensure time-focusing geometry [17,18]. In front of the recoil-ion detector, the ions were accelerated by about 2 keV over a 2 mm gap onto the MCPs. The scattered and charge exchanged He^0 projectiles were detected downstream by another position-sensitive channel-plate detector. The main He^{1+} beam was deflected after penetrating the target and dumped into a Faraday cup. The vacuum in the beam line and scattering chamber (without gas target) was typically 2×10^{-8} Torr. With infusing N_2 target gas (target pressure about 3×10^{-5} Torr) the pressure in the scattering chamber was slightly above 10^{-7} Torr. Thus, the ratio of the charge-exchanged beam resulting from the interaction with the rest gas to that from the interaction with the target gas was less than 1/10. The detected projectiles provided the zero-time signal, i.e. the time when the fragmentation occurred accompanied by capture into the projectile. The uncertainty in the time zero resulted mainly from the time resolution of the detector and the intersection length of the target with the He^{1+} beam and it was typically 2 ns.

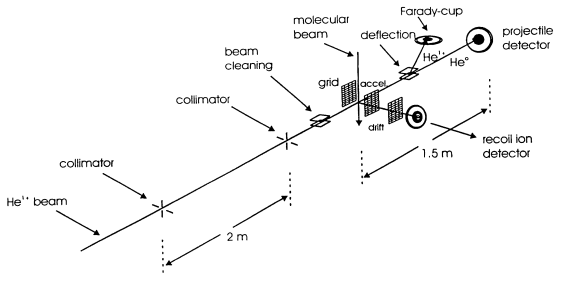

Fig. 1. Experimental set-up.

3. The multi-hit-delay-line-anode detector

The recoil-ion detector consists of a two MCPs and a delay-line-anode. The MCPs provide signals well separated from noise that can be used as a timing signal for the arrival of the recoil-ion on the detector. The position information is obtained from a delay-line-anode [19–21]. The delay-line-anode is composed of two crossed double wire planes spirally wound over a copper plate where they are held with ceramic holders fixed on the edges of the copper plate in order to isolate the wires from one another and from the copper plate. The distance is about 1 mm between the wire planes and 1 mm between the copper plate and the near wire plane. Each wire plane consists of a pair of wires with nearly 0.5 mm distance to separate them from each other. A slightly different potential is applied to the positive-signal wire (p-signal wire) and the negative-signal wire (n-signal wire). The two wire planes are rotated by 90° with respect to each other in order to provide the position of an ion in two dimensions (see Fig. 2). The electron avalanche produced by an ion hitting the MCPs passes through the wires of the anode. Two signals are produced from a short drop of the voltage on each delay line wire when the electron avalanche passes. The time of the occurrence of the signal on each end (arrival time) is measured relative to the event signal from the MCPs. The x- or y-position

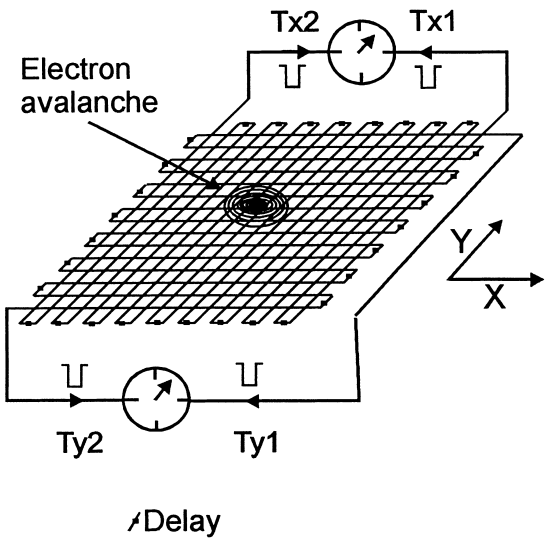

Fig. 2. Two position planes and the function principle of the delay-line-anode. The delays is obtained just from the length of the wire turns. The Clocks represent time measurements.

of an ion can be measured in two ways from the delay-line-anode (for example x-direction):

1. Through measuring the time difference on the delay line between the two x-signals obtained from opposite ends of the delay line.
2. Through measuring the time of a signal from one end of the x-delay-line relative to the absolute time of the event signal from the MCPs.

In order to obtain a position resolution better than 0.1 mm, a time resolution better than 50 ps is required in measuring the time of the signals on the ends of the delay-lines. This was achieved by applying different voltages to the p-signal wire (+700 V) and the n-signal wire (+500 V). The difference of the electronic signals from the wire ends of each pair of the delay line in one dimension is amplified using a fast differential preamplifier. A time resolution better than 50 ps was obtained from the signals at each end of the x- and y-delay-lines using differential amplifiers. The total delay time over the whole delay-line structure was about 30 ns. Thus for 50 mm diameter active detection area a position resolution better than 0.1 mm is feasible.

Since only Time to Digital Converters (TDCs) with a single-hit capability were used, it was necessary to insert a fast switch device which directs signals consecutive in time from one output to separate TDC-stop inputs. Thus a delay-gate signal is created from the first pulse (5 ns delay and 1 μs gate). The direct signal and the delayed gate signal are created from the first pulse. The direct signals and the delayed gate signal are fed into a logical "And" gate "overlap coincidence". From this unit one obtains a timing-signal for the second pulse. More similar circuits can be added to allow the processing of a third and fourth multi-hit. The time to resolve two consecutive signals is presently limited to 5 ns. This limit comes from the limited pulse length because of the electronic modules used.

The delay-line detector and the delay-line wire system can in principle detect and separate the signals of two recoil-ions impacting the detector in a very short time difference within the limited time resolution of the system (50 ps) if they impact at different positions. Whether the TOF and position for both fragments can be determined, depends only on the electronics used. With commercially standard fast timing modules we were able to separate recoil impacts, which were separated by a time delay of more than 5 ns.

If two recoil-ions hit the detector within 30 ns (i.e. the total signal processing time on the delay line), the x- and y-delay-line signals of the two particles interfere with each other. However, the sum of the corresponding arrival times for each ion on opposite ends of a delay-line is constant for a true event, because the delay line has always a constant length for each signal pair. This information can be used to sort the signals of all the particles according to their arrival time and thus their position on the detector can be identified.

A schematic of the electronic set-up of the multi-hit-detector-system is shown in Fig. 3 for the detection of the two N^{q+}-fragments in a triple coincidence with the He^0-projectile. The signal from the MCPs is processed by a fast timing amplifier and a constant fraction unit providing the digital signal of the arrival time of an ion on the detector. A "coincidence signal" of the first recoil-ion with the projectile provides the start signal of the data processing. The position of an ion is obtained by measuring the time difference between

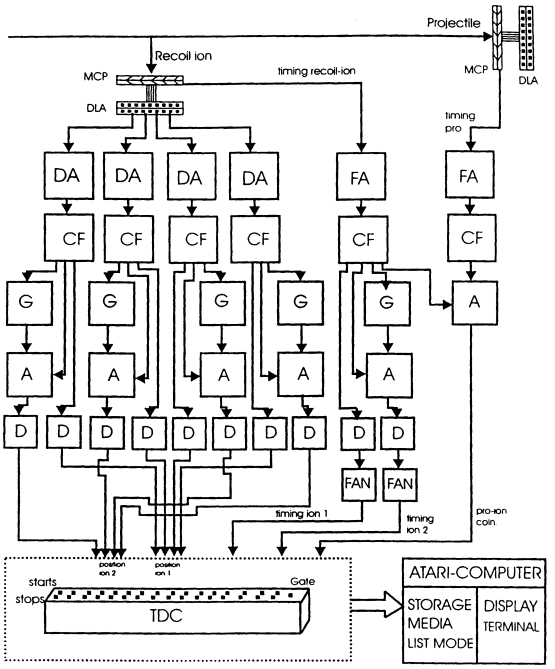

Fig. 3. Electronic set-up of the position-sensitive multi-hit-detector-system. The different shorts mean the following. DA: difference amplifier, CF: constant fraction, G: Gate and delay unit, A: coincidence module, FAN: Fan in/out module, D: cable delay and TDC: time to digital converter.

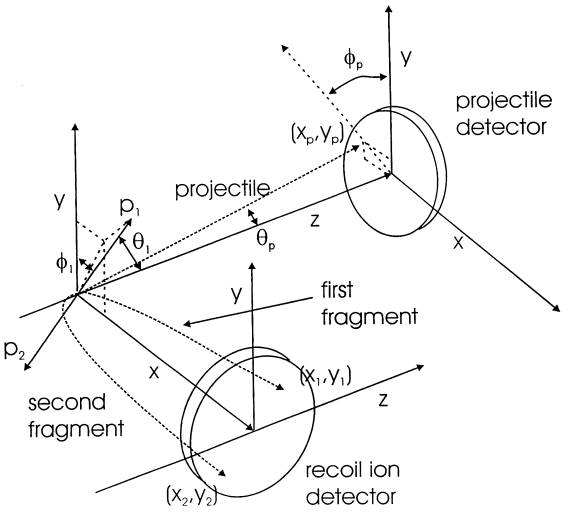

Fig. 4. Kinematics picture of the collision process where the momentum vectors of projectile, first recoil-ion and second recoil-ion are presented in Cartesian and spherical coordinates with the different measured momentum components and angles.

the signals from x- and y-delay lines relative to the start signal from the MCPs. The time and position of the second fragment is obtained from coincidence circuits as described in the previous paragraph.

4. Kinematics of the recoil-ion detection after Coulomb-explosion

Using PMDS-technique the momentum vectors of all charged ionic fragments are determined from the TOF (in x-direction) and position (y,z) on the detector as shown in Fig. 4. The relation between the total TOF of fragment i (TOF_i) with a mass m_i and charge state q_i can be calculated from the relation:

$$\mathrm{TOF}_i = \frac{p_{xi} - p_{xi}^0}{F(q_i)} + \frac{m_i d}{p_{xi}}. \tag{1}$$

$F(q_i)$ is the electrical force on the ion at the interaction site, p_{xi}^0 the initial momentum component in the field direction, p_{xi} is the momentum component in the direction of the field at the end of the acceleration region and d is the drift length.

If the initial momentum components of fragment (i) $(p_{xi}^0, p_{yi}^0, p_{zi}^0)$ are all zero, the fragments will be detected at (y_0, z_0) in the center position of the detector and t_0 is equal to the center position of the corresponding peak in the TOF spectrum of the corresponding charge state (see Fig. 5). Thus the deviations (first order) in the TOF_i i.e. $\Delta t_i = t_i - t_0$ and in the position $\Delta y_i = y_i - y_0$ and $\Delta z_i = z_i - z_0$ yield direct information on the intial momentum components $(p_{xi}^0, p_{yi}^0, p_{zi}^0)$ according to Eqs. (2)–(4), respectively.

$$p_{xi}^0 \approx F(q_i)\Delta t_i, \tag{2}$$

$$p_{yi}^0 \approx \frac{m_i\,\Delta y_i}{\mathrm{TOF}_i}, \tag{3}$$

$$p_{zi}^0 \approx \frac{m_i\,\Delta z_i}{\mathrm{TOF}_i}. \tag{4}$$

Now, we will consider a general dissociation process of a molecule into n fragments. Assuming

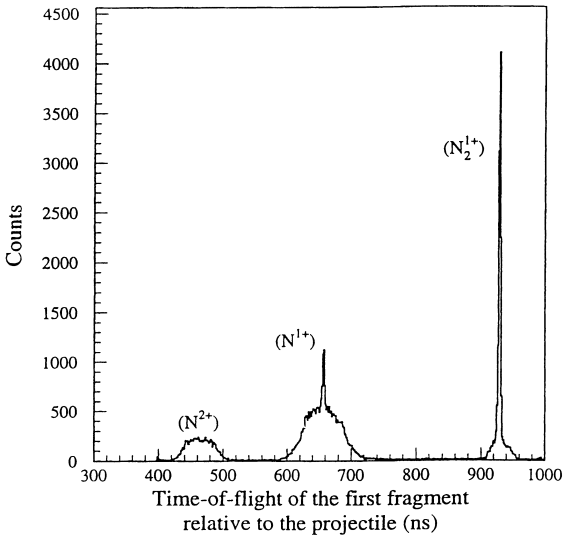

Fig. 5. Time-of-flight of the molecular ions and atomic fragments relative to the projectile.

that the dissociation process takes place instantaneously, the sum of the time deviations and position deviations along each axis for all fragments vanishes because of momentum conservation:

$$\sum_{i=1}^{n} a_i \, \Delta t_i - \Delta p_{x\mathrm{pro}} = 0, \tag{5}$$

$$\sum_{i=1}^{n} b_i \, \Delta y_i - \Delta p_{y\mathrm{pro}} = 0, \tag{6}$$

$$\sum_{i=1}^{n} c_i \, \Delta z_i - \Delta p_{z\mathrm{pro}} = 0, \tag{7}$$

where a_i, b_i and c_i are the transformation factors of the time deviation and position deviations into momentum units, respectively, which are experimentally determined. The change of the projectile momentum ($\Delta p_{x\mathrm{pro}}, \Delta p_{y\mathrm{pro}}, \Delta p_{z\mathrm{pro}}$) is typically small compared to the momentum from the Coulomb fragmentation and can be in a very good approximation neglected. The orientation of the initial molecule and thus the emission vectors of the fragments with respect to the projectile direction can be estimated from the measured momentum vector components (see Fig. 4).

5. Test measurement: dissociation of N_2

To test the spectrometer system and the multi-hit capability of the detector we have investigated the fragmentation process of N_2 by swift He^{1+} impact. The major reaction channels resulting from the collision process are:

$$He^{1+} + N_2 \rightarrow He^0 + N_2^{1+}, \tag{8}$$

$$He^{1+} + N_2 \rightarrow He^0 + N^0 + N^{1+}, \tag{9}$$

$$He^{1+} + N_2 \rightarrow He^0 + N^{p+} + N^{q+} + (p+q-1)e^-. \tag{10}$$

A typical TOF spectrum (integrated over all positions) for the first arriving recoil-ion measured relative to the projectile impact is shown in Fig. 5. The TOF of an ion depends on q according to $\sqrt{m/q}$. The different peaks result from different ions or ionic fragments of the molecule (N_2). The fragments (N^{1+}, N^{2+}, N^{3+}, etc.) resulting from the dissociation of the molecule show a broad TOF distribution because of the kinetic energy gained through the Coulomb-explosion (0–120 eV). These are fragments with a momentum up to nearly 475 a.u. The N_2^{1+} peak is "sharp" because its width reflects mainly the experimental resolution (reaction channel of Eq. (8)). The narrow peak superimposed on the wide N^{1+} peak results from fragmentation of N_2 in N^{1+} plus N^0 which leads to low energy ions (reaction channel of Eq. (9), etc.).

In Fig. 6, a two-dimensional spectrum of the TOF of the first fragment measured with respect to the projectile time against that of the second fragment measured with respect to the projectile time is displayed. The true events are scattered along diagonal lines resulting from the correlation in the TOF between the two fragments from the two-body Coulomb explosion process of the charged fragments of a dissociating molecule according to Eq. (4). For the two-body Coulomb-explosion, the charged fragments explode in opposite directions because of the repulsive Coulomb force between the charged fragments and negligible momentum transfer from the projectile onto the dissociating fragments. Thus the sum of their TOFs of the fragments from an

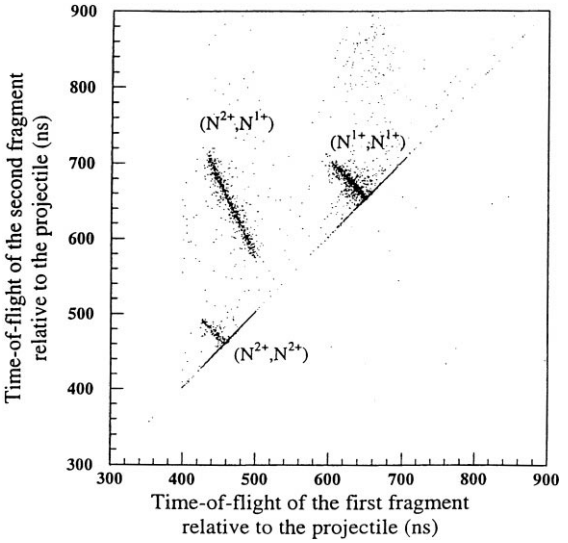

Fig. 6. Time-of-flight of the first fragment relative to the projectile against that of the second fragment relative to the projectile.

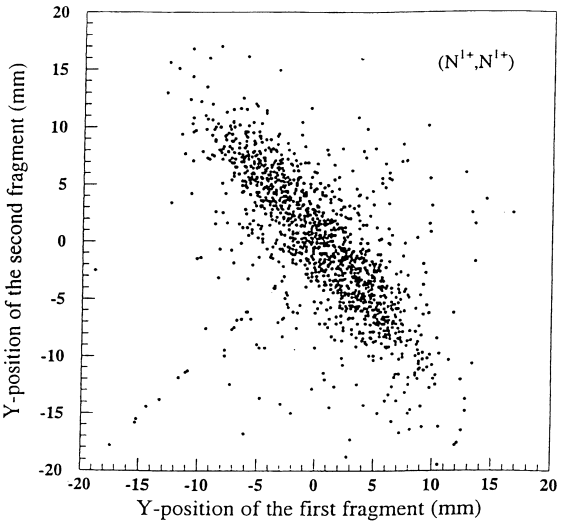

Fig. 7. The position of the first fragment against that of the second fragment on the detector in the same direction along the y-axis when the molecule explodes in similar charged states.

ion pair relative to the time of the collision measured by the arriving time of the projectile weighted to $\sqrt{q/m}$ is constant. The different diagonal lines result from the Coulomb explosion of the molecule into different charge-state pairs as indicated near each diagonal line in Fig. 6.

The position of the first fragment versus that of the second fragment on the detector in the y-direction is displayed in Fig. 7. From Eq. (6), it is easy to derive for a two-body fragmentation process that the position of the first fragment y_{R1} and the second fragment y_{R2} on the recoil ion detector in the y-direction must have a linear relation to each other. If both fragments are similar i.e. have the same charge state and mass, the sum of their positions for example in y-direction must be equal to a constant ($2y_0$). In a two-dimensional plot of y_{R1} and y_{R2} the correlated fragments must therefore fall on a diagonal line (see Fig. 7). Within the limited experimental resolution of the system the position of the correlated fragments fall indeed on the diagonal line.

Another important check is the angular correlation of the emitted fragments in the Coulomb-explosion of the molecule. The emission angle of a fragment from the dissociation of the molecule can be calculated from the measured momentum components. For the two-body fragmentation of N_2 the difference between the azimuthal angles (ϕ_{R1} and ϕ_{R2}) (see Fig. 4) of the first and the second

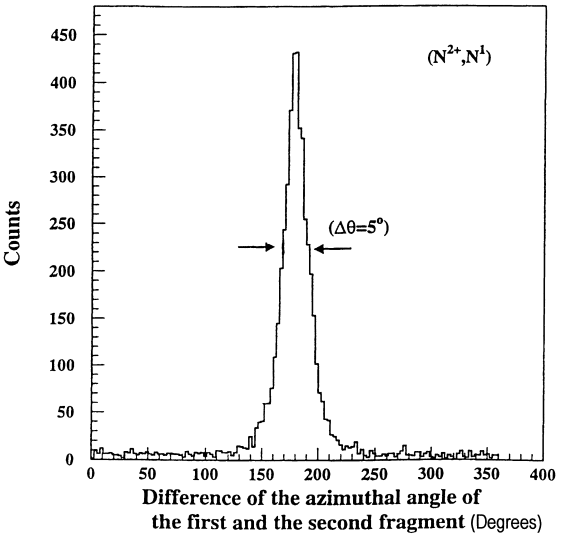

Fig. 8. The difference between the azimuthal angles of the first fragment ϕ_1 and second fragment ϕ_2 represented in the range from 0° to 360°.

fragments is displayed in Fig. 8. The derived distribution peaks at 180°. The width at half-maximum of the peak at 180° in Fig. 8 is ±5° which gives the angular resolution of the system for the N-fragments.

The resolution of the system depends on several factors: the dominant contributions are due to the time and position resolution of the detectors, the spatial width of the gas target and the field homogeneity inside the spectrometer. The momentum resolution of the system can be estimated from Eqs. (2) and (3) for each direction separately.

In the x-direction (field direction), an uncertainty of the measured time of flight results from the time resolution of projectile and recoil-ion detectors (for each one about 850 ps) and the intersection range of the gas target with the collimated beam. Using a spectrometer with a time focusing geometry [17,18], the width of 0.2 mm of the intersection range has a negligible influence on the TOF of the recoil-ions. For the present geometry the calculated resolution of the TOF of 1 ns for the fragments of the N_2 corresponds to a momentum resolution of 3.2 a.u. In the y-direction the measured position is uncertain to 0.2 mm because of the intersection width of the beam. An overall position resolution in the y-direction of 0.2 mm corresponds to a momentum resolution of 5 a.u. applying a high extraction field in order to have a high efficiency to detect the fragments from the Coulomb-explosion of N_2. In the z-direction, the target is extended along the beam direction and thus results in a large uncertainty in Δz. However, the z_0 position (i.e. the center-of-mass between two Coulomb-exploding fragments) can be calculated from the detected position on the detector.

The field conditions inside the spectrometer are crucial to the linearity of the momentum measurement in the TOF and position direction. They are slightly distorted by the non-homogeneity in the extraction field caused by the needle. This problem can be easily overcome if a supersonic gas jet [17,18] is used as the target. Another advantage of using a gas jet is that one obtains a very small spatial intersection range between the gas target and the projectile. In this case the momentum resolution can be improved by more than a factor of 10.

The sum of the momentum components of both fragments measured in the present experiment resulting from the Coulomb-explosion of N_2 in one direction ($p_{x1} + p_{x2}$ and $p_{y1} + p_{y2}$) calculated from the TOF (x-direction) and the position (y-direction) is displayed in Fig. 9 (a) and (b), respectively. From the width at half

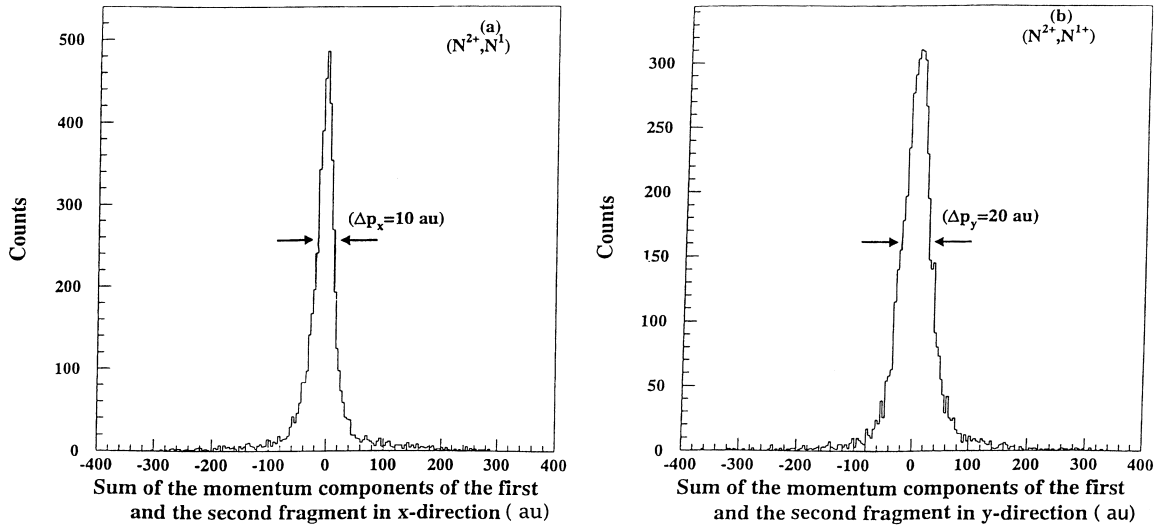

Fig. 9. The sum of the momentum components for both fragments derived from the TOF in the x-direction (a) and the position on the recoil ion detector (perpendicular to the beam direction) in the y-direction (b), respectively.

maximum a momentum resolution of 10 and 20 a.u. is obtained for the momentum components measured from the TOF and position in the y-direction, respectively. The factor of two between the estimated and measured momentum resolutions results probably from a small non-homogeneity in the extraction field.

In the following we are going to discuss in detail the different parameters that affect the efficiency of the system. The efficiency of the detected fragments is influenced by the limited transparency of the grids (two grids with nearly 95% optical transmission for each) that they have to cross from the collision position to the detector. The limited geometrical efficiency of the MCPs (two MCPs with nearly 80% efficiency for each) which is determined by the channel wall size affects the total efficiency of the detection of the impacting particles. Thus the system has a maximum efficiency of nearly 58% to detect a single particle because of the geometrical limits. Detecting an ion pair in coincidence leads to an efficiency of 33% and the detection of three particles in coincidence lead to a total efficiency of nearly 20% and so on. Another factor that affect the efficiency of the MCP is the energy and the charge state of the impacting particles because the ionization cross section of the primary electrons emitted from the walls of the MCP depends on these parameters. However, a high voltage (800 V per MCP) applied on the MCPs provides a saturation electron emission from the pack side of the MCPs set in Chevron-order for each impacting charged particle.

The charged fragments are detected generally with a high efficiency of a total solid angle of nearly 4π up to a certain energy by projecting them on the detectors with high extraction fields. However, the fragments with a high kinetic energy release particularly these emitted within an angular range $\Delta\phi$ nearly perpendicular to the extraction field are not projected on the position sensitive detector and one needs in this case extremely high extraction fields. In this case, the fragments are projected on the detector and detected with high efficiency of nearly 100% if their energy is less than a certain energy value. Beside the strength of the extraction field and mass of the fragments, this energy depends on the charge state of the fragments, for example N^{1+} are detected with a high efficiency of nearly 100% of 4π solid angle if their $E_\perp \leqslant 30$ eV ($\approx p_\perp \leqslant 240$ a.u.) and N^{2+} with $E_\perp \leqslant 42.3$ eV ($\approx p_\perp \leqslant 285$ a.u.) for the field and geometry of the spectrometer used in this test experiment and mentioned previously.

The two-pulse-resolution (10 ns) of the multi-hit-detector system influence the efficiency of the detected fragments. Because the fragments are separated and sorted into different hits according to their arrival times, the momentum information about the fragments that reach the detector in the dead time is lost. In the case of diatomic molecules, ion pairs with different charge states arrive at the detector with a time difference longer than the time resolution needed to resolve two consecutive hits. In the case of similar charge states the time difference of the arrival of both fragments on the detector is very short and depends on the emission angle relative to the extraction field. Similar charged fragments emitted perpendicular to the extraction field arrive at the same time on the detector and in this case the position and TOF are measured for the first hit and are lost for the second hit. This effect causes a limitation on the efficiency to detect multi-hit particles with similar mass and charge state for example in this experiment N^{1+}-fragments were detected with nearly 70% form 4π assuming isotropic angular distribution of the emitted fragments.

The effect of the limitation of the efficiency because of the two-pulse-resolution is tested by displaying the transversal momentum of both fragments in the case of the dissociation of N_2 into similar charged fragments (two N^{1+}) in Fig. 10. Since similar charged ion pairs are separated and sorted by the difference in their TOF, the fragment emitted in the direction of the detector arrives first and the fragment emitted away from the detector arrives as a second hit. Thus momentum space of the first fragment (a) shows nearly a semi-circle which lies in the direction of the recoil ion detector while the second fragment (b) show an opposite semi-circle which lies away from the detector as shown in Fig. 10. The gap in the semi-circle of the transversal momentum represents the event lost because of the efficiency effect of the double-pulse resolution. This effect causes a gap of $\Delta\phi = 30^\circ$

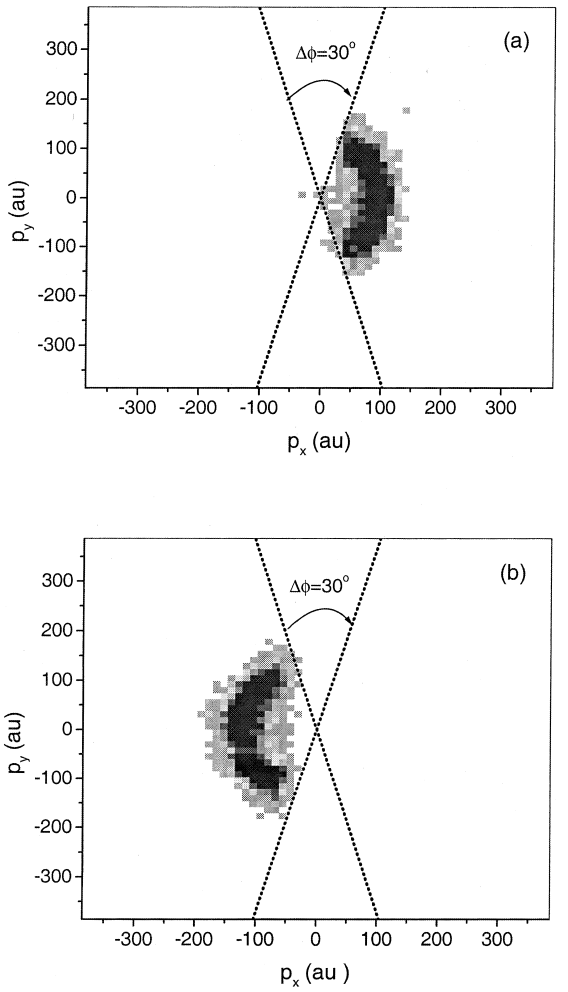

Fig. 10. p_x vs p_y in a.u. for the first fragment (a) and the second fragment (b) emitted from the dissociation of N_2 into a similar charged ion pair in this case $2N^+$.

from the complete ϕ range of 180° which causes a detection a lost of 30% of the emitted fragments assuming isotropic emission.

6. Conclusions

A position sensitive multi-hit detector system has been developed to detect all fragments resulting from the dissociation of a molecule. The characteristics of this new technique can be summarized as follows:

1. All charged fragments from a molecular dissociation process can be projected and detected with a high efficiency of nearly 4π solid angle up to a certain kinetic energy release by applying strong enough extraction fields thus guaranteeing that the majority of the dissociation events be detected . However, the detection efficiency of the system is limited by the geometry of the components of the spectrometer and detector and the technical effects of the electronics mentioned previously leading to an overall efficiency of nearly 20% for three particles in coincidence.
2. For an event where both fragments are detected, the momentum vector for each fragment is completely derived from the TOF and the position on the recoil ion detector.
3. The present system has a momentum resolution of 10 and 20 a.u. (see Fig. 9(a) and (b)) for the momentum components of N_2 fragments to which a momentum of up to 500 a.u. is imparted in the dissociation measured from the TOF and the y-position on the detector, respectively. The angular resolution for the azimuthal angles of the fragments calculated from the measured momentum components is about $\pm 5°$ (see Fig. 8). With a cold supersonic gas jet target a momentum resolution can be improved by more than a factor of 10 due to the significantly improved position resolution.

This position sensitive multi-hit detector system is a versatile and powerful technique to study the structure and the dynamics of the dissociation of simple and complex molecules in the collision process with photons, electrons or ions through measuring complete momenta for all outgoing charged particles in all channels. The molecular structure can be studied by measuring the energy, emission angle and the determination of the electronic structure of the Coulomb-exploding fragments resulting from the different dissociation channels of the original molecule. Furthermore, determining the trajectory of the projectile with respect to the molecular axis allows the investigation of the anisotropy of emission of fragments from the exploding molecule relative to the scattering angle of the projectile [22].

This new technique of the PMDS is not limited to the detection of charged fragments resulting

from the dissociation of molecules but can be applied also to the detection of all charged particles from a many-particle system such as all electrons ejected in multiple-ionization processes. In this case, many electrons can be detected with a high efficiency of 4π solid angle for soft electrons with an energy lower than 100 eV and complete information about their momenta can be recorded thus providing a superior method to study the dynamics and correlation effects of multiple-ionization processes and many-particle-systems to a high possible degree of differentiality.

Acknowledgements

This work was supported by DEG, BMFT, GSI, DOE and the Division of Chemical Sciences. Two of us (I. Ali and K. Khayyat) acknowledge the support by DAAD. R. Doerner was supported by the Feodor Lynen Program of the Alexander von Humboldt Stiftung, V. Mergel by the Studienstiftung des Deutschen Volkes.

References

[1] G. Dugardin, S. Lenach, O. Dutuit, P.-M. Gyon, M. Richard-Viard, Chem. Phys. 88 (1984) 339.
[2] F.B. Yousif, B.G. Lindsay, C.J. Latimer, J. Phys. B: At. Mol. Phys. 23 (1990) 495.
[3] A.K. Edwards, R.M. Wood, M.F. Steuer, Phys. Rev. A 15 (1977) 48.
[4] R.M. Wood, A.K. Edwards, M.F. Steuer, Phys. Rev. A 15 (1977) 1433.
[5] A.K. Edwards, R.M. Wood, J. Chem. Phys. 23 (1990) 1491.
[6] B. Brehm, G. de Frenes, Int. J. Mass. Spectrom. Ion Phys. 26 (1978) 251.
[7] Z. Vager, D.S. Gemmell, B.J. Zabransky, Phys. Rev. A 14 (1976) 638.
[8] D.S. Gemmell, E.P. Kanter, W.J. Pietsch, Chem. Phys. Lett. 55 (1978) 331.
[9] D.S. Gemmell, Chem. Rev. 80 (1980) 301.
[10] J.H.D. Eland, Mol. Phys. 61 (3) (1987) 725.
[11] M.J. Besnard, L. Hellner, G. Dujardin, D. Winkoun, J. Chem. Phys. 88 (1988) 1732.
[12] I. Ben-Itzhak, S.G. Ginther, K.D. Carnes, Nucl. Instr. and Meth. B 66 (1992) 401.
[13] R. Moshammer, GSI scientific report, Darmstadt, Germany, 1993.
[14] I. Ali, Scientific Report, Institut für Kernphysik, Frankfurt, Germany, 1994.
[15] J. Becker, K. Beckord, U. Werner, H.O. Lutz, Nucl. Instr. and Meth. B 337 (1994) 49.
[16] U. Werner, K. Beckord, J. Becker, H.O. Folkerts, H.O. Lutz, Nucl. Instr. and Meth. B 98 (1995) 385.
[17] V. Mergel, R. Dörner, J. Ullrich, O. Jagutzki, S. Lencinas, S. Nüttgens, L. Spielberger, M. Unverzagt, C.L. Cocke, R.E. Olson, M. Shulz, U. Buck, E. Zanger, W. Theisinger, M. Isser, S. Geis, H. Schmidt-Böcking, Phys. Rev. Lett. 74 (1995) 2200.
[18] J. Ullrich, R. Dörner, V. Mergel, O. Jagutzki, L. Spielberger, H. Schmidt-Böcking, Mol. Phys. 30 (5) (1994) 285.
[19] S.E. Sobottka, M.B. Williams, IEEE Trans. Nucl. Sci. NS-35 (1988) 348.
[20] H. Keller, G. Klingelhöfer, E. Kankeleit, Nucl. Instr. and Meth. A 258 (1987) 221.
[21] J.H.D. Eland, Meas. Sci. Technol. 5 (1995) 1501.
[22] I. Ali et al., to be published.